BIOCELL
2020 44(4): 671-681

Tech Science Press

Allicin neuroprotective effect during oxidative/inflammatory injury involves AT1-Hsp70-iNOS counterbalance axis

Luciana MAZZEI[1,2]; María Belén RUIZ-ROSO[3]; Natalia DE LAS HERAS[3]; Sandra BALLESTEROS[3]; Carolina TORRES-PALAZZOLO[4]; León FERDER[5]; Alejandra Beatriz CAMARGO[4]; Walter MANUCHA[1,2,*]

[1] Instituto de Medicina y Biología Experimental de Cuyo (IMBECU), Consejo Nacional de Investigaciones Científicas y Tecnológicas (CONICET), Mendoza, 5500, Argentina
[2] Área de Farmacología, Departamento de Patología, Facultad de Ciencias Médicas, Universidad Nacional de Cuyo Centro Universitario, Mendoza, 5500, Argentina
[3] Departamento de Fisiología, Facultad de Medicina, Universidad Complutense, Madrid, 34523, España
[4] IBAM, Universidad Nacional de Cuyo, CONICET, Facultad de Ciencias Agrarias, Mendoza, M5528AHB, Argentina
[5] Department of Pediatrics, Nephrology Division, Miller School of Medicine, University of Miami, Miami, 33012, USA

Key words: Allicin, neuroinflammation, BV-2 cells, AT1 receptors, iNOS, Hsp70

Abstract: The ancestral cultures have described many therapeutic properties of garlic; therefore, it is of central interest to elucidate the molecular basis explaining this millenary empirical knowledge. Indeed, it has been demonstrated a neuroprotective effect of allicin–a phytochemical present in garlic- linked to oxidative-inflammatory modulation. Allicin improved neuronal injury by heat shock protein 70 (Hsp70) and inducible nitric oxide synthase (iNOS) regulation. Also, allicin exerts renal protection involving a possible angiotensin type 1 receptor (AT1) interaction. In connection, AT1 overexpression has been recognized as a central deleterious factor in many brain diseases. However, there are no studies that evaluate AT1-Hsp70-iNOS interaction as a mechanism linked to neuroinflammation. Thus, our central aim is to evaluate if the allicin protective effect is associated with an AT1-Hsp70-iNOS counterbalance axis. For this study, a murine microglial cell line (BV-2) was injured with lipopolysaccharides and treated or not with allicin. Then, it was evaluated cell viability, proinflammatory cytokine levels, cellular oxidative stress, iNOS, Hsp70, and AT1 protein expression (cellular and mitochondrial fractions), nitrite levels, and protein-protein interactions. The results demonstrated that allicin could prevent neuronal injury due to a reduction in oxidative stress and inflammatory status mediated by an AT1-Hsp70-iNOS counterbalance axis linked to direct protein-protein interaction.

Introduction

A Recently, there are a lot of reports on the use of so-called functional foods and their implications for human health, where most of these studies refer to cardiovascular pathology (Lonnie *et al.*, 2020). Specifically, allicin (Alli) -an organosulfur compound obtained from garlic- exhibits a potent antihypertensive effect through vasodilatory properties (Cui *et al.*, 2020). Also, Alli was effective in wound healing in an experimental diabetes model (Toygar *et al.*, 2020). In addition, Alli plays an important role in regulating energy homeostasis, which provides a promising potential therapy for obesity and metabolic disorders (Zhang *et al.*, 2020). However, it draws our attention that these alternative tools are less explored in other pathologies of increasing global expansion, such as those developed at the level of the central nervous system (CNS). Recently has been demonstrated a neuroprotection promissory effect of allicin (Alli) -an organosulfur compound obtained from garlic- linked to modulation of the oxidative stress, inflammation, and apoptosis (Kong *et al.*, 2017; Lv *et al.*, 2015). In close connection, diallyl trisulfide -another specific organosulfur compound obtained from garlic- showed anti-neuroinflammatory properties in lipopolysaccharide (LPS)-stimulated BV-2 microglia (Ho and Su, 2014). This finding stimulates us to deepen the knowledge of pathophysiological aspects of neurological disorders as well as the development of neurodegenerative diseases, and possibly to contribute with new information for therapeutic approaches.

In this context, our laboratory and others discussed a central hypothesis on neurotoxicity due to a close

*Address correspondence to: Walter Manucha, wmanucha@yahoo.com.ar
Received: 06 September 2020; Accepted: 13 October 2020

Doi: 10.32604/biocell.2020.014175

relationship between glutamatergic toxicity with altered mitochondrial function and increased oxidative stress (Goracci *et al*., 2010; Manucha, 2017; Son and Elliott, 2014). Indeed, all these factors are widespread during the neuronal apoptosis present in multiple chronic, inflammatory, and neurodegenerative pathologies of the central nervous system (Chabrier *et al*., 1999; Urrutia *et al*., 2014) where the nitric oxide (NO) is a predominant effector of neurodegeneration. In addition, the loss of an adequate mitochondrial function has been related to alterations in calcium homeostasis and changes in the glutamatergic pathway (Brown and Vilalta, 2015; Takarada *et al*., 2013; Smaili *et al*., 2011). To emphasize cell death is essential for the suitable development and maintenance of the central nervous system; whereas, its mismatch has been described in patients with neurodegenerative processes associated with oxidative stress (Pchelina *et al*., 2014; Pinazo-Durán *et al*., 2015).

It has recently been recognized that mitochondrial dysfunction and NO levels would be responsible for many processes of neurological toxicity, at least in part. Consequently, a new finding closely related has been discussed. More specifically, the authors suggest that inducible nitric oxide synthase (iNOS) is modulated by heat shock protein 70 (Hsp70) expression (Zlatković *et al*., 2014). In close connection, Hsp70 is a suitable marker of cellular injury in the nervous system after a neurotoxic stimulus (Rajdev and Sharp, 2000). Therefore, loss in the Hsp70 function linked to NO overproduction could contribute to the development and maintenance of neurodegenerative disorders (Nakamura and Lipton, 2007). To reinforce, Liu and colleagues induced a cellular injury with glutamate in the *in vitro* spinal cord model. More specifically, the Alli treatment significantly attenuated neuronal death by decrease iNOS expression with a significantly increased in the Hsp70 expression (Liu *et al*., 2015). Parallelly, it was reported -in chronic kidney disease- that Alli exerts protection like to an angiotensin II receptor inhibitor (AT1) losartan, and *in silico* analyses supported the notion that Alli and losartan could have a common mechanism involving interaction with AT1 (García *et al*., 2017). These results are particularly interesting since it is known that AT1 overexpression has been recognized as a central and early deleterious factor in the development of many brain diseases and, consequently, angiotensin receptor blockers (ARBs) are outstanding candidates for the treatment of brain disorders (Saavedra, 2017).

Collectively, we proposed to evaluate the following key hypothesis: Alli prevents neuronal injury in the murine microglial cell line -a cellular model of neurotoxicity- due to a reduction in oxidative stress/inflammation mediated by an AT1-Hsp70-iNOS counterbalance axis. If this is so, Alli may exert a critical and fundamental anti-inflammatory/anti-oxidative role in neurological disorders as well as the development of neurodegenerative diseases. In addition, we also assessed whether this counterbalance axis is associated with mitochondrial dysfunctions.

Materials and Methods

A cell culture and treatment

The BV-2 cells, a murine microglial cell line provided by Centro Trasfusionale Banca Biologica and Cell Factory IRCCS AOU (San Martino, IST L.go R. Benzi, 10 16132 Genoa, Italy), were cultured in RPMI 1640. The medium was supplemented with 10% FBS, 100 U/mL penicillin, 100 µg/mL streptomycin in an atmosphere of 95% air, and 5% CO_2 at 37°C. The trypan blue method was used to determine the number of viable cells (millions/mL). The protocols were started after 24 h of cellular quiescence with 0.1% of FBS. BV-2 cells were injured or not with lipopolysaccharides (LPS, 100 ng/mL), and BV-2 cells injured with LPS and were co-treated or not with Alli (50 µM) for 72 h. The culture medium containing the LPS, Alli, or both, was replaced every day. Each protocol (triplicate) was replicated five to ten times. The treatments lasted 3 days, and finally, the cells were collected to perform the specific determinations.

Alli specifications

Alli was synthesized by oxidation of diallyl disulfide (DADS) with hydrogen peroxide following the previously reported by the group (González *et al*., 2007). The synthesized Alli were further isolated and purified by fractions collection after HPLC separation using a normal phase Waters Spherisorb S5W HPLC column and hexane: isopropanol (92:8 v/v) as mobile phase. Then, collected fractions were concentrated under reduced pressure and characterized by UV-spectroscopy and GC-MS analyses. UV spectra were obtained by using a Varian's Cary 50 UV-Vis Spectrophotometer, and quantification was carried out by using the extinction coefficient (Lawson and Hughes, 1991). For GC-MS analyses, a Perkin Elmer Clarus 500 was used. Alli was confirmed by UV and mass spectra; the last, through the confirmation of formed vinyldithiins. Obtained mass and UV spectra agree with the bibliography (Lawson and Hughes, 1991; Ilić *et al*., 2012). Synthesized Alli was preserved in a closed amber vial at −80°C (Locatelli *et al*., 2014).

Cell viability

The cell viability was performed by the MTT technique. Concisely, upon completion of the pharmacological treatment, BV-2 cells were loaded with MTT to a final concentration of 1 mg/mL and incubated for 3 h at 37°C. The chromogen formed was dissolved in DMSO, and the optic density (OD) value measured at 570 nm was used to index cell viability. The absorbance of the untreated BV-2 cells (Control) was also measured in order to calculate relative cell viability (in percentage).

Proinflammatory cytokine levels

Proinflammatory cytokines levels were evaluated in the culture medium by ELISA kit. TNF-α (ab208348, ABCAM) and IL-1β (EK0394, Boster Biological Engineering and Cloud-Clone Corp) values were determined according to the manufacturer's instructions.

Measure for cellular oxidative stress

After the pharmacological treatments, the fluorescent dye dihydroethidium technique was performed to assess the superoxide anion ($O_2^{\bullet-}$) production according to a previous report without any modifications (Martínez-Martínez *et al*., 2016). The levels of the superoxide anion are presented as

an n-fold increase over the values of the control group. These correspond to three assays, and each one was done for quintuplicate.

Procedure to isolate mitochondria from BV-2 cultures

Cells (2×10^6) were added 5 mL of buffer (protease inhibitor cocktail, 70 mM sucrose, 1 mM EDTA, 200 mM mannitol, and 10 mM HEPES pH 7.4; Sigma, St. Louis, MO). The BV-2 cells were homogenized with a Dounce glass homogenizer (Wheaton, catalog no. 357544). The lysate was processed according to a previous report (Prado *et al.*, 2018). Finally, we evaluate the purity of the mitochondrial fraction obtained according to O'Beirne and Williams (1988).

NADPH activity assay

NADPH oxidase activity was measured in BV-2 cells and the mitochondrial fractions of the BV-2 cells by means of the Luminol (521-31-3, Sigma-Aldrich) technique, and where all the procedures and reagents used were the same as previous reports (Prado *et al.*, 2018). The results were expressed as arbitrary fluorescence units (AFU) per microgram of protein and minute of incubation.

iNOS, Hsp70 and AT1 protein expression by western blot technique

Protein expressions were measured both in BV-2 cells and the mitochondrial fractions of the BV-2 cells. For both cases, all procedures and reactions were the same as those used in previous reports (Manucha and Vallés, 2008). The primary antibodies used were: iNOS (sc-7271 mouse monoclonal, dilution 1:2500), Hsp70 (sc-33575 rabbit polyclonal, dilution 1:1000), and AT1 (sc-31181 goat polyclonal, dilution 1:1000). For cellular fraction, the housekeeping gene expression was performed with anti-β-actin (sc-47778 mouse monoclonal antibody, dilution 1:2000). For mitochondrial fraction, the housekeeping gene expression was performed with anti-COX IV (ab-16056 rabbit polyclonal antibody, dilution 1:1500). The ratios of the immunosignal were standardized to 1 for the corresponding control values (BV-2 cells and mitochondrial fractions without treatment).

Immunofluorescence confocal microscopy

Cellular fixation, cryoprotection, as well as the permeabilization procedures, were according to García *et al.* (2012). The primary and secondary antibodies used, as well as the processes and equipment, were the same as those used in previously reported work by our laboratory. For details, refer to García *et al.* (2014).

Determination of nitrite levels in BV-2 cells

We measured nitrite levels by Griess reaction. Homogenates from lysed BV-2 cells were processed according to a previous report (Mazzei *et al.*, 2010). The nitrites levels were determined by a spectrophotometer (540 nm). Results were expressed as nmol of nitrite generated per μg protein per 100 μL homogenate.

Protein-protein interactions by immunoprecipitation technique

The immunoprecipitation was performed in BV-2 cells injured or not with LPS and treated or not with Alli during 72 h to assess the possible physical interaction between iNOS, Hsp70, and AT1. We carried out all procedures for western blot technique as well as immunoprecipitation according to previously published reports (García *et al.*, 2012). iNOS and AT1 expressions were adjusted to Hsp70 protein expression for all experimental conditions, and results were expressed as a ratio. Finally, for guaranteed specificity of immune-precipitation through anti-Hsp70 antibody, entire fractions were incubated with normal rabbit immunoglobulin; and as a result, Hsp70 was not immune-precipitated under any conditions (data not shown).

Statistical analysis

ANOVA II and Bonferroni post-test were used for the analysis of the data. We considered a $p < 0.05$ as significant. The results as the means ± SEM were processed by using GraphPad Software, Inc., USA.

Results

Morphology and cell viability

Fig. 1 shows the morphological variations happening in BV-2 cells activation subsequent to LPS treatment (LPS). On the contrary, BV-2 cells without treatment (Control) exhibited the typical ramified morphology of inactive microglia. However, simultaneous treatment with LPS plus Alli (LPS+Alli) attenuated the LPS-induced microglial activation; and consequently, BV-2 cells returned to display the distinctive ramified cellular structure of inactive microglia.

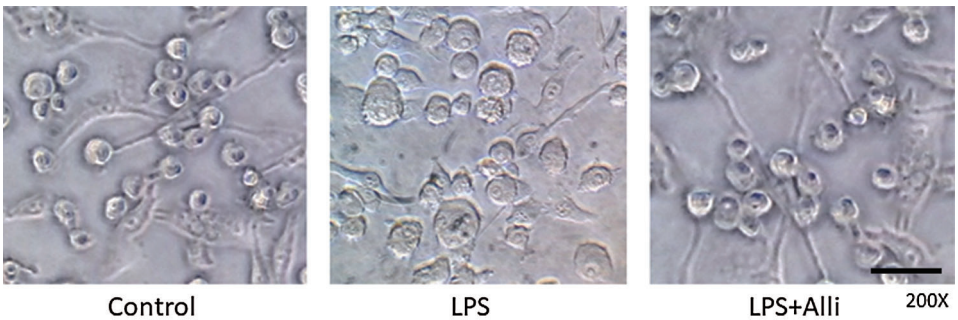

FIGURE 1. Effects of Allicin on LPS-induced microglia activation. Microscopy images are presented and showing the morphology from control BV-2 cells (Control), LPS-treated BV-2 cells (LPS), and LPS-treated BV-2 cells co-treated with Allicin (LPS+Alli). The cells were swelled, and the nucleus was prominent, whereas allicin exposure attenuated LPS-induced cellular changes. Images showed from one experiment and representative of at least five independent experiments. Scale bar: 50 μm.

The MTT assay showed that LPS at the final concentration of 100 ng/mL resulted in a reduction in mean cell viability of BV-2 microglia (80 ± 5 *vs.* 100 ± 10; LPS *vs.* Control; $p < 0.05$). Meanwhile, the treatment with Alli had a positive effect on the viability of BV-2 cells. Specifically, BV-2 cells were protected from the injury induced by LPS (95 ± 8 *vs.* 80 ± 5; LPS + Alli *vs.* LPS; $p < 0.05$) (Fig. 2). In addition, treatment only with Alli did not modify the cell morphology or viability when compared to control BV-2 cells (data not shown).

Oxidative stress and inflammatory response linked to NADPH oxidase activity in BV-2 cells

ROS production linked to NADPH oxidase activity is a key microglial response that often leads to neuronal toxicity. In this sense, and since NADPH oxidase activity contributes to the neurotoxicity/neuroinflammation associated with LPS, we investigated if Alli might reduce microglial NADPH oxidase activity and the following ROS production in BV-2 cells injured by LPS. As results, LPS caused a significant increase in NADPH oxidase activity after 72 h of stimulation (15000 ± 1500 *vs.* 10000 ± 1000; LPS *vs.* Control; $p < 0.01$); while co-treatment with Alli (LPS+Alli) reduced NADPH oxidase activity, returning it almost to the control (12000 ± 1000 *vs.* 15000 ± 1500; LPS+Alli *vs.* LPS; $p < 0.05$) (Fig. 3A). Additionally, according to the evidence that mitochondria are the main source of ROS production, we demonstrate that mitochondrial NADPH oxidase activity was significantly higher in LPS treatment than it was in the control cells (12000 ± 1200 *vs.* 8000 ± 1500; LPS *vs.* Control; $p < 0.01$). On the contrary, the mitochondrial fraction from BV-2 cells Alli-treated showed a lower NADPH oxidase activity compared to mitochondrial fraction from BV-2 cells with LPS-treated (10000 ± 1000 *vs.* 12000 ± 1200; LPS+Alli *vs.* LPS; $p < 0.05$) (Fig. 3B).

Consistently, in DHE assay, the fluorescence intensity was higher in LPS-treated BV-2 cells than in control (200 ± 10 *vs.* 100 ± 10; LPS *vs.* Control; $p < 0.01$), suggesting higher levels of $O_2^{\bullet-}$ during LPS-induced microglial activation. However, the treatment with Alli prevented the altered $O_2^{\bullet-}$ production in the LPS-induced microglial activation (130 ± 20 *vs.* 200 ± 10; LPS+Alli *vs.* LPS; $p < 0.01$) (Fig. 3C). The Alli treatment alone did not modify levels of $O_2^{\bullet-}$ in control cells (data not shown).

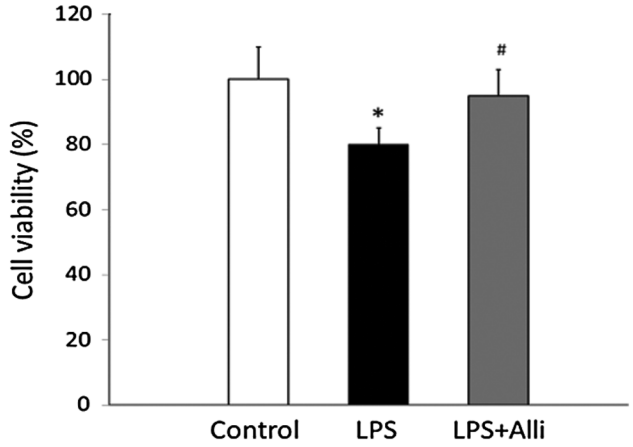

FIGURE 2. BV-2 cells viability. Control bar represents viability (%) in 72 h of control BV-2 cells. LPS bar represents viability (%) in 72 h of LPS-treated BV-2 cells. The LPS+Alli bar represents viability (%) in 72 h of LPS-treated BV-2 cells co-treated with Allicin. The results were expressed as means ± SEM of 5 independent observations. $^{*}p < 0.05$ *vs.* Control, and $^{\#}p < 0.05$ *vs.* LPS.

Parallelly, the pro-inflammatory cytokine levels were determined in the culture medium from BV-2 cells. Tab. 1 shows that both TNF-α, as well as IL-1β levels, were significantly increased in the culture medium of LPS-treated BV-2 cells (1500 ± 100 *vs.* 110 ± 20 and 150 ± 20 *vs.* 50 ± 10; LPS *vs.* Control; $p < 0.001$ and $p < 0.01$; TNF-α and IL-1β levels, respectively). However, the treatment with Alli significantly inhibited the production of TNF-α as well IL-1β (500 ± 50 *vs.* 1500 ± 100 and 100 ± 20 *vs.* 150 ± 20; LPS+Alli *vs.* LPS; $p < 0.001$ and $p < 0.05$; TNF-α and IL-1β levels, respectively).

Allicin effects on AT1, Hsp70, iNOS expression and nitrite levels in BV-2 cells

Firstly, we demonstrated a higher iNOS protein expression from BV-2 cells treated with LPS (LPS) related to BV-2 cells without treatment (Control) (2.5 ± 0.2 *vs.* 1.00 ± 0.1; LPS *vs.* Control; $p < 0.001$). Conversely, after 72 h of Alli treatment, decreased iNOS protein levels were shown in BV-2 cells co-treated with LPS (LPS+Alli) compared to LPS alone (LPS) (1.5 ± 0.4 *vs.* 2.5 ± 0.2; LPS+Alli *vs.* LPS; $p < 0.01$) (Fig. 4). The immunofluorescence analyses reinforce results from western blot iNOS protein expression (Fig. 5). In addition, increased nitrite levels were shown in BV-2 cells treated with LPS (LPS) compared to non-treated BV-2 cells (Control) (200 ± 15 *vs.* 100 ± 10 nmol NO_2 generated/μg protein/100 μL homogenate; LPS *vs.* Control; $p < 0.001$). Alli treatment reduced nitrite levels in BV-2 cells co-treated with LPS (LPS+Alli) compared to LPS alone (LPS) (130 ± 15 *vs.* 200 ± 15 nmol NO_2 generated/μg protein/100 μL homogenate; LPS+Alli *vs.* LPS; $p < 0.01$) (Fig. 6). In a second step, and to validate/compare our protocol—respect to previous findings—on the relationship between the iNOS and Hsp70 proteins as well as the Alli effect on these, we simultaneously tested the Hsp70 expression. In this sense, we found lower Hsp70 level in BV-2 cells treated with LPS (LPS) compared to non-treated BV-2 cells (Control) (0.2 ± 0.1 *vs.* 1.00 ± 0.15; LPS *vs.* Control; $p < 0.001$). Contrariwise, after Alli treatment, an increased Hsp70 protein levels were shown in BV-2 cells co-treated with LPS (LPS+Alli) compared to LPS alone (LPS) (0.6 ± 0.1 *vs.* 0.2 ± 0.1; LPS+Alli *vs.* LPS; $p < 0.01$) (Fig. 4). Parallel, we proceeded to determine the AT1 protein levels. In the same way as what is established for iNOS, we found a higher AT1 level in BV-2 cells treated with LPS (LPS) related to BV-2 cells without treatment (Control) (3 ± 0.2 *vs.* 1.00 ± 0.09; LPS *vs.* Control; $p < 0.001$). While, after Alli treatment, a decreased AT1 protein levels were shown in BV-2 cells co-treated with LPS (LPS+Alli) compared to LPS alone (LPS) (1.8 ± 0.3 *vs.* 3 ± 0.2; LPS+Alli *vs.* LPS; $p < 0.01$) (Fig. 4). All these results were confirmed by immunofluorescence assays (Fig. 5).

To highlight, we were able to demonstrate that protein expressions -in mitochondrial fractions- were consistent with cellular expressions. More specifically, as shown in

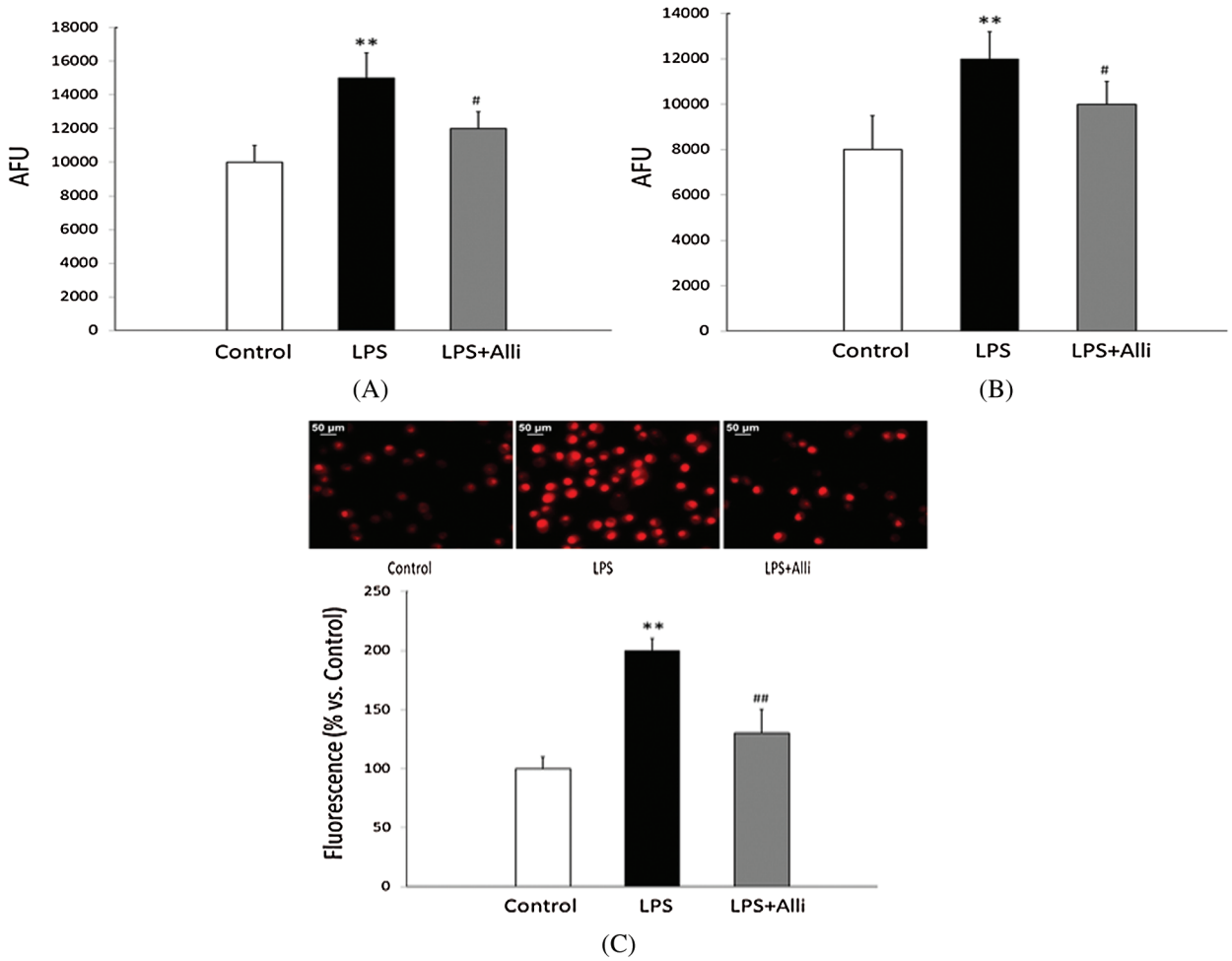

FIGURE 3. Oxidative stress in LPS-injured BV-2 cells: Allicin effect. A-NADPH oxidase activity in BV-2 cells. Control bar represents NADPH oxidase activity (arbitrary fluorescence units, AFU) in 72 h of control BV-2 cells. LPS bar represents NADPH oxidase activity (AFU) in 72 h of LPS-treated BV-2 cells. The LPS+Alli bar represents NADPH oxidase activity (AFU) in 72 h of LPS-treated BV-2 cells co-treated with Allicin. The results were expressed as means ± SEM of 5 independent observations. $^{**}p < 0.01$ *vs.* Control, and $^{\#}p < 0.05$ *vs.* LPS. B-NADPH oxidase activity in mitochondrial fractions from BV-2 cells. Control bar represents NADPH oxidase activity (AFU) from the mitochondrial fraction in 72 h of control BV-2 cells. LPS bar represents NADPH oxidase activity (AFU) from the mitochondrial fraction in 72 h of LPS-treated BV-2 cells. The LPS+Alli bar represents NADPH oxidase activity (AFU) from the mitochondrial fraction in 72 h of LPS-treated BV-2 cells co-treated with Allicin. The results were expressed as means ± SEM of 5 independent observations. $^{**}p < 0.01$ *vs.* Control, and $^{\#}p < 0.05$ *vs.* LPS. C-Superoxide anion production in BV-2 cells. Upper panel: Representative microphotographs of control BV-2 cells (Control), stimulated with LPS (LPS), and stimulated with LPS in presence of Allicin (LPS+Alli) labeled with DHE. Lower panel: Control bar represents the quantification of superoxide anions in 72 h of control BV-2 cells. LPS bar represents the quantification of superoxide anions in 72 h of LPS-treated BV-2 cells. The LPS+Alli bar represents the quantification of superoxide anions in 72 h of LPS-treated BV-2 cells co-treated with Allicin. The results were expressed as means ± SEM of 5 independent observations. $^{**}p < 0.01$ *vs.* Control, and $^{\#\#}p < 0.01$ *vs.* LPS.

TABLE 1

Effects of Allicin on pro-inflammatory cytokine production in BV-2 cells. The results were expressed as means ± SEM of 5 independent observations. $^{***}p < 0.001$ and $^{**}p < 0.01$ *vs.* Control; and $^{\#\#\#}p < 0.001$ and $^{\#}p < 0.05$ *vs.* LPS.

Treatments	Pro-inflammatory cytokines	
	TNF-α (pg/mL)	IL-1β (pg/mL)
Control	110 ± 20	50 ± 10
LPS	1500 ± 100***	150 ± 20**
LPS + Alli	500 ± 50###	100 ± 20#

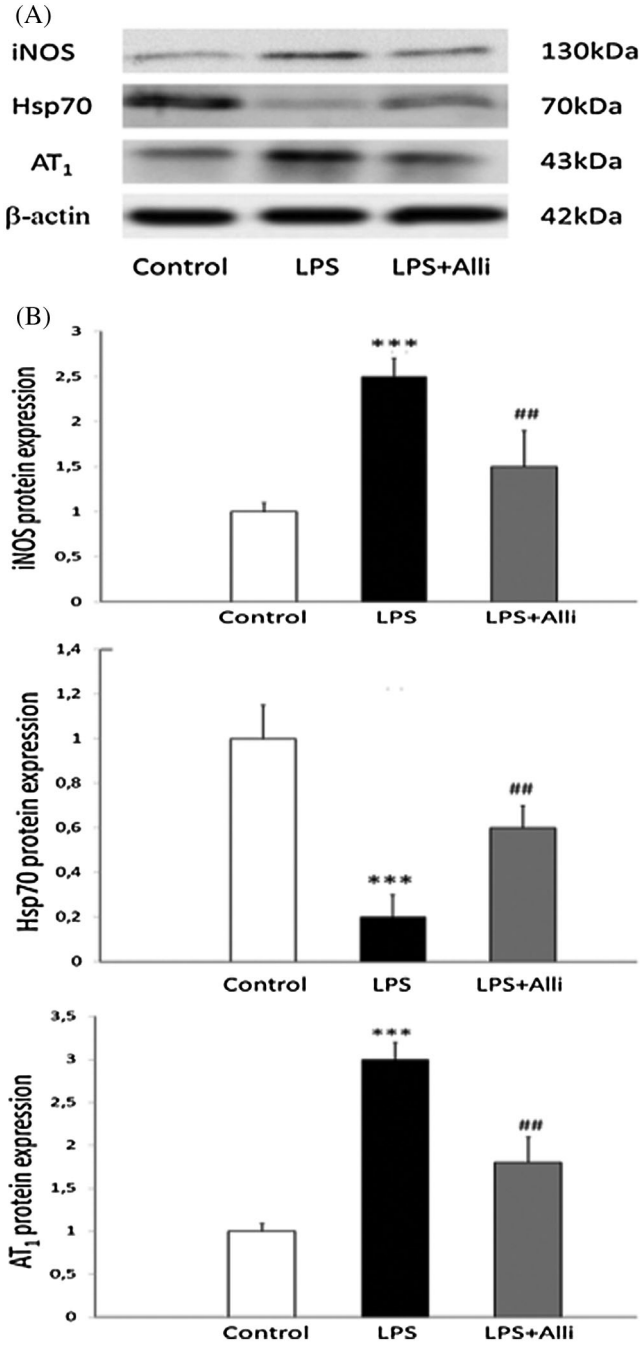

FIGURE 4. Allicin effects on AT1, Hsp70, iNOS expression by western blot technique in BV-2 cells. (A) Representative blot of AT1, Hsp70, and iNOS proteins expression in control BV-2 cells (Control), stimulated with LPS (LPS) and stimulated with LPS in the presence of Allicin (LPS+Alli). The β-actin protein expression–as a housekeeping gene–is shown in the same order as the densitometry bars. (B) The levels of AT1, Hsp70, and iNOS proteins were established after normalization of the appropriate control: 1. The results were expressed as means ± SEM of 5 independent observations. $^{***}p < 0.001$ *vs.* Control, and $^{\#\#}p < 0.01$ *vs.* LPS.

Fig. 7, we established a higher mitochondrial iNOS protein expression from BV-2 cells treated with LPS (LPS) related to BV-2 cells without treatment (Control) (2.0 ± 0.1 *vs.* 1.00 ± 0.2; LPS *vs.* Control; $p < 0.001$). Conversely, after Alli treatment, a decreased in the iNOS protein level was shown in BV-2 cells co-treated with LPS (LPS+Alli) compared to LPS alone (LPS) (0.9 ± 0.1 *vs.* 2.0 ± 0.1; LPS + Alli *vs.* LPS; $p < 0.001$).

Concurrently we tested the mitochondrial Hsp70 protein expression. In this sense, we found lower mitochondrial Hsp70 level in BV-2 cells treated with LPS (LPS) related to BV-2 cells without treatment (Control) (0.2 ± 0.1 *vs.* 1.00 ± 0.15; LPS *vs.* Control; $p < 0.001$). Inversely, after Alli treatment, increased mitochondrial Hsp70 protein levels were shown in BV-2 cells co-treated with LPS (LPS+Alli) compared to LPS alone (LPS) (0.6 ± 0.1 *vs.* 0.2 ± 0.1; LPS +Alli *vs.* LPS; $p < 0.01$). Parallelly, we found a higher mitochondrial AT1 expression in BV-2 cells treated with LPS (LPS) related to BV-2 cells without treatment (Control) (2.3 ± 0.2 *vs.* 1.00 ± 0.1; LPS *vs.* Control; $p < 0.001$). While, after Alli treatment, decreased mitochondrial AT1 protein levels were shown in BV-2 cells co-treated with LPS (LPS +Alli) related to LPS alone (LPS) (1.2 ± 0.1 *vs.* 2.3 ± 0.2; LPS + Alli *vs.* LPS; $p < 0.001$). With special attention to the effect produced by Alli and as a result of the comparison between mitochondrial versus cellular protein expressions, emerge a more significant impact at the mitochondrial level. To highlight, treatment only with Alli did not modify AT1, Hsp70, iNOS expression, and nitrite levels in BV-2 cells when compared to control BV-2 cells (data not shown).

iNOS-Hsp70-AT1 interactions in BV-2 cells

To further evaluate the possible interaction between iNOS-Hsp70 as well as AT1-Hsp70, coimmunoprecipitation was performed. Moreover, we also assess the hypothesis that Hsp70 would be less associated with iNOS and with AT1 after treatment with Alli in BV-2 cells LPS-stimulated.

Cellular extracts from BV-2 cells (Control, LPS, and LPS+Alli) were immunoprecipitated with the Hsp70 antibody and analyzed to evaluate the presence of coprecipitated proteins iNOS as well as AT1. Relevant for our study, we verify the interactions of iNOS-Hsp70 and AT1-Hsp70 under Control and experimental conditions (LPS and LPS+Alli) (Fig. 8). Our second finding was that the LPS treatment produced a significant increase in the iNOS-Hsp70 as well AT1-Hsp70 ratios in relation to proteins ratio from untreated BV-2 cells (5.2 ± 0.6 *vs.* 1.0 ± 0.1 and 4.3 ± 0.5 *vs.* 1.0 ± 0.2; LPS *vs.* Control; $p < 0.001$).

The third instance of our study was to delineate whether Alli could be implicated in the iNOS, AT1, and Hsp70 proteins interactions. In this sense, we established that the Alli co-treatment in LPS-stimulated BV2 cells produced a significant decrease in the iNOS-Hsp70 as well AT1-Hsp70 ratios with respect to proteins ratio from LPS-treated BV2 cells (1.5 ± 0.4 *vs.* 5.2 ± 0.6 and 1.8 ± 0.6 *vs.* 4.3 ± 0.5; LPS + Alli *vs.* LPS; $p < 0.01$) (Fig. 8).

Discussion

In the present work, anti-inflammatory/neuroprotective proprieties of Alli were demonstrated in LPS-stimulated BV2 microglia, as well as one new possible mechanism by which Alli exerts its effects. As neuroinflammation is a crucial process in the pathophysiology of many chronic neurodegenerative and neuropsychiatric diseases, a deep understanding of the underlying molecular mechanisms is needed (Kong *et al.*, 2017).

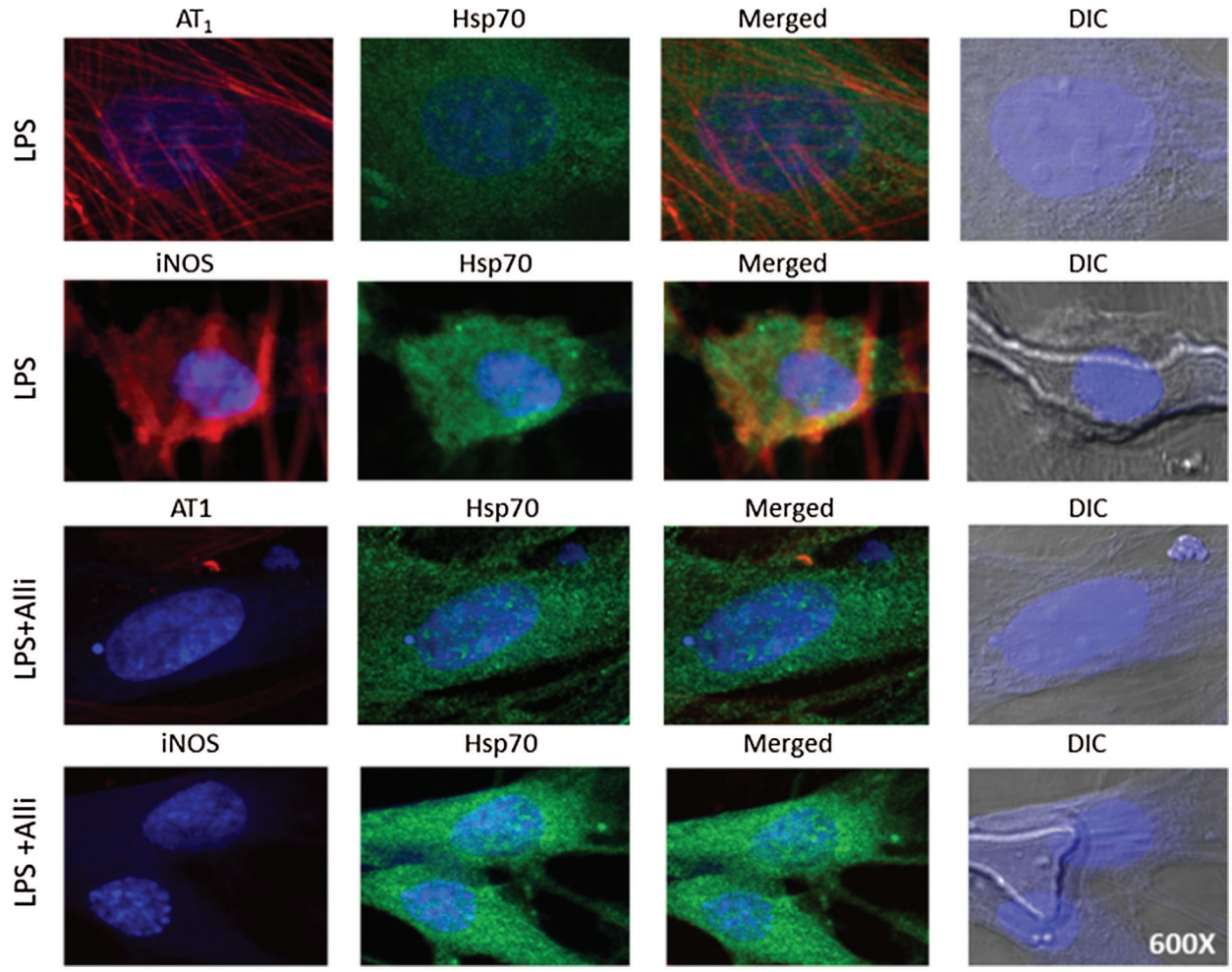

FIGURE 5. Allicin effects on AT1, Hsp70, iNOS expression by immunofluorescence technique in BV-2 cells. Immunofluorescence of AT1, Hsp70, and iNOS in BV-2 cells stimulated with LPS (LPS), and in BV-2 cells stimulated with LPS in the presence of Allicin (LPS+Alli). Colors reference: AT1 and iNOS (red), Hsp70 (green), and Hoechst 33342 stained nucleus (blue). Column 4 shows the merged images of the differential interference contrast image (DIC) and Hoechst 33342 stained nucleus (blue). Images are representative of five different experiments. Magnification 600X.

Of interest, among the functional foods, garlic (*Allium sativum* L., family Liliaceae) contains rich sulfur-containing amino acids, and it has been used as important traditional Chinese medicine (Farooqui and Farooqui, 2018). In addition, it was also demonstrated there is topical use of the allicin and alliin (Toygar *et al.*, 2020; Sardari *et al.*, 2006).

If fresh garlic is chopped or crushed, alliin (the most abundant free amino acid in garlic) gets in contact with the enzyme alliinase that converts alliin to diallyl-dithiosulfinate (Alli). Alli could cross the blood–brain barrier, and several studies evidence its anti-inflammatory/neuroprotective, antidepressant, and pro-cognitive actions (Xiang *et al.*, 2017; Zhang *et al.*, 2018; Mocayar Marón *et al.*, 2020). However, not all the molecular mechanisms that justify such protective effects are fully understood.

The microglial cells show an extremely versatile behavior; that is the reason why the structure is in intimate relation to its phagocytic function (Kettenmann *et al.*, 2011). In this sense, the present study demonstrates, for the first time, the effect of Alli on the morphology of microglial cells. Resident microglial cells (also known as "resting microglia") can transform after LPS from a ramified form to an amoeboid form and acquire a proinflammatory phenotype (Fernández-Arjona *et al.*, 2017). Alli attenuated the LPS-induced microglial activation and, consequently, BV-2 cells return to exhibit the typical ramified morphology of resident microglia. Indeed, the phenotypic microglial morphology recovery by Alli treatment could be related to changes in cytoskeletal proteins. In close connection, a recent proteomic analysis showed that Alli produces post-translational modifications of type S-thioallylation in various proteins, including proteins related to actin filaments (Gruhlke *et al.*, 2019). Moreover, Alli induces disruption of the actin cytoskeleton in mouse fibroblasts. However, the fibroblasts lost their actin-dependent extensions and showed a mostly spheroidal morphology. An altered dynamic of Actin affects the proinflammatory activity of the microglia stimulated by LPS (e.g., reduced NO secretion, iNOS expression, and reduced release of TNF-α and IL-6) (Uhlemann *et al.*, 2016). In the same way, we have shown in BV2 LPS-injured cells that Alli can modulate the NO levels, iNOS expression, proinflammatory cytokines, oxidative stress, as well as AT1 expression.

The renin-angiotensin-aldosterone system (RAAS) emerges as a possible target of the Alli mechanism of action

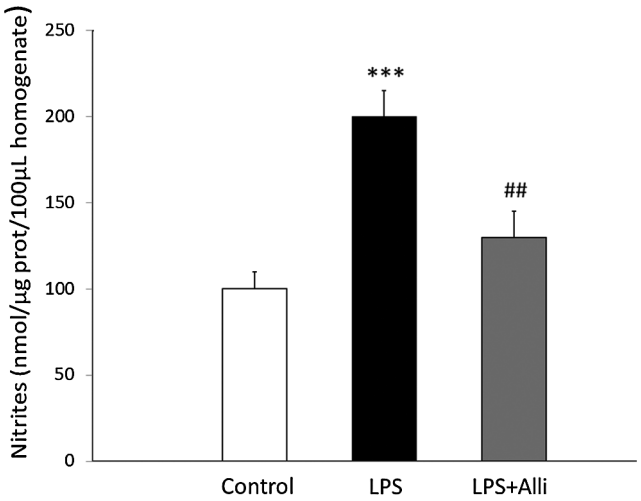

FIGURE 6. Allicin effects on nitrite levels in BV-2 cells. Measurement of nitrite generated (nmol NO_2 generated/µg protein/100 µL homogenated). Control bar represents the quantification of nitrite in 72 h of control BV-2 cells. LPS bar represents the quantification of nitrite in 72 h of LPS-treated BV-2 cells. The LPS+Alli bar represents the quantification of nitrite in 72 h of LPS-treated BV-2 cells co-treated with Allicin. The results were expressed as means ± SEM of 5 independent observations. $^{***}p < 0.001$ *vs.* Control, and $^{\#\#}p < 0.01$ *vs.* LPS.

since it plays a crucial role in microglial polarization, and Angiotensin II (via AT1 receptor and NADPH activation) induce a pro-inflammatory microglial phenotype (Labandeira-Garcia *et al.*, 2017). RAAS over-activation has been associated with inflammation and mitochondrial dysfunction. Here, and of particular interest, we show -in total cellular lysate as well as in mitochondrial fraction from BV2 cells- that LPS increases the expression of AT1 and iNOS, while Alli was capable of reversing these effects. Consistently, *in silico* modeling and docking analysis suggests that Alli might act as a potent AT1 antagonist even more effective than losartan (García *et al.*, 2017).

Microglia has a variety of functions in the brain, including synaptic pruning, CNS repair, and mediating the immune response. Depending on the magnitude of the injury, microglia can contribute to host defense and repair. Microglia can transform into proinflammatory/classically activated (M1) or anti-inflammatory/alternatively activated (M2) phenotypes following environmental signals related to physiological conditions or lesions (such as LPS). As previously mentioned, several recent studies have shown interactions between the brain RAAS and different factors involved in microglial polarization. The locally formed angiotensin is involved in local pathological changes of these tissues and modulates immune cells, which are equipped with all the RAAS components. Metabolic reprogramming has recently been involved in the regulation of the neuroinflammatory response. Interestingly, it was recently observed a mitochondrial RAAS, which is altered in aged brains. Dysregulation of brain RAAS plays a significant role in aging-related changes and neurodegeneration by exacerbating oxidative stress and neuroinflammation, which may be attenuated by pharmacological manipulation of RAAS components (Labandeira-Garcia et al., 2017). In this

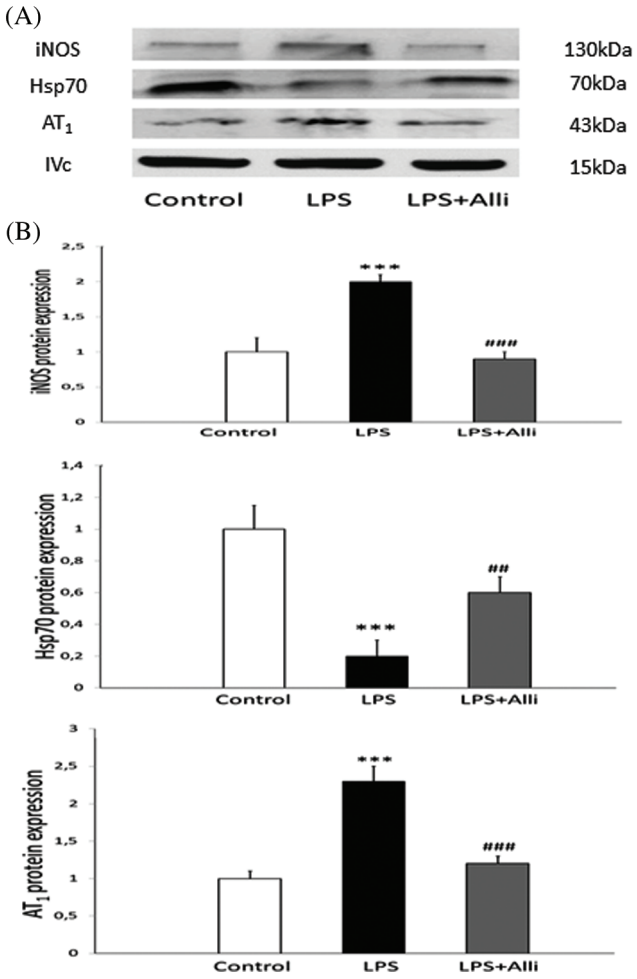

FIGURE 7. Allicin effects on AT1, Hsp70, iNOS expression by western blot technique in mitochondrial fractions from BV-2 cells. (A) Representative blot of AT1, Hsp70, and iNOS proteins expression in the mitochondrial fraction from: control BV-2 cells (Control), stimulated with LPS (LPS), and stimulated with LPS in the presence of Allicin (LPS+Alli). Expression levels of the mitochondrial electron transport complex IVc (Complex IVc)–as a housekeeping gene–is shown in the same order as the densitometry bars. (B) The levels of AT1, Hsp70, and iNOS proteins were established after normalization of the appropriate control: 1. The results were expressed as means ± SEM of 5 independent observations. $^{***}p < 0.001$ *vs.* Control, $^{\#\#}p < 0.01$, and $^{\#\#\#}p < 0.001$ *vs.* LPS.

sense, our results are consistent with the current literature because Alli could modulate the local immune response involved in tissue reaction after LPS injury due to a lower expression of AT1 receptors (both at the cellular level and at the mitochondrial level) associated with AT1-Hsp70-iNOS counterbalance axis. Interestingly, Alli modulates the lymphocytes' immune response via scavenger receptors (Toma *et al.*, 2019); in close connection, the scavenger receptors are downregulated by the RAAS. In detail, the phosphatidylinositol 3-kinase/Akt/FoxO1 pathway participates in angiotensin II suppression of hSR-BI/CLA-1 expression and suggests that the RAAS downregulates the endothelial receptor for hSR-BI/CLA-1. (Yu *et al.*, 2007). Alli attenuates LPS-induced acute injury via the PI3K/Akt pathway (Wang *et al.*, 2018). Also, Alli inhibited

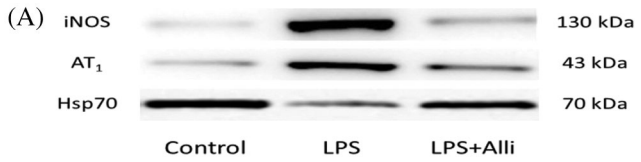

(B)

iNOS/Hsp70	1.0±0.1	5.2±0.6 ***	1.5±0.4 ##
AT_1/Hsp70	1.0±0.2	4.3±0.5 ***	1.8±0.6 ##
	Control	LPS	LPS+Alli

FIGURE 8. iNOS-Hsp70-AT1 protein-protein interactions in BV-2 cells. (A) Representative blot of the cellular extracts from BV-2 cells (Control, LPS, and LPS+Alli) immune-precipitated with Hsp70 antibody and coprecipitated with iNOS as well as AT1 proteins. (B) Cellular extracts from BV-2 cells (Control, LPS, and LPS+Alli) were immune-precipitated with Hsp70 and coprecipitated for AT1 or iNOS. The data as ratios, express levels of AT1 and iNOS coprecipitating with Hsp70. The results were expressed as means ± SEM of 5 independent observations. $^{***}p < 0.001$ *vs.* Control, and $^{\#\#}p < 0.01$ *vs.* LPS.

interleukin-1β (IL-1β) induced overproduction of NO, iNOS, prostaglandin E2, and cyclooxygenase-2, as well as pro-inflammatory cytokines tumor necrosis factor-alpha and interleukin-6 in a dose-dependent manner by PI3K/Akt/NF-κB downregulation (Qian *et al.*, 2018).

On the other hand, as previously mentioned, mitochondrial dysfunction and NO levels would be responsible for many processes of neurological toxicity; and in agreement, Hsp70 may protect by downregulation of iNOS protein expression (Zlatković *et al.*, 2014); in where Hsp70 could be considered as a suitable marker of cellular injury in the nervous system after a neurotoxic stimulus. To highlight, our present findings have shown an Hsp70 lower expression after LPS stimulation, and the opposite happened (according to Liu *et al.*, 2015) in the cells co-treated with Alli. Moreover, and for the first time, stress markers, as well as total cellular protein expressions, were consistent with mitochondrial fractions. These results could suggest that Alli could contribute to the restoration of mitochondrial dynamics.

In order to evaluate the anti-inflammatory properties of Alli, pro-inflammatory cytokine levels and oxidative biomarkers were measured in BV-2 cells after treatment with LPS. As previously mentioned and consistent with the data published in the literature (Ho and Su, 2014), the treatment with Alli significantly inhibited the production of TNF-α, IL-1β, nitrites as well as the NADPH oxidase activity. Reinforcing our results, Alli also decreases the levels of proinflammatory mediators after LPS treatment in other cell types as chondrocytes (Qian *et al.*, 2018), human umbilical vein endothelial cells (Zhang *et al.*, 2017), and lung cells (Zheng *et al.*, 2014), among others.

Finally, our findings led us to consider the possibility of protein–protein interaction as part of the protective mechanism Alli-mediated. The potential physical interaction between iNOS, Hsp70, and AT1 proteins was done by immunoprecipitation in BV-2 cells injured with LPS treated or not with Alli. As outstanding results, we find first that there are interactions between the proteins AT1-Hsp70 and iNOS-Hsp70, second and fundamental to our hypothesis that these protein interactions are altered in BV2 cells LPS-injured. While on the contrary, Alli can reverse protein interactions. New studies should deepen the knowledge about protein interactions associated with changes in their cellular functions.

Together and based on the finding showed above, we suggested that Alli avoids the neuronal injury in BV2 cells -a cellular model of neurotoxicity- by a reduction in oxidative stress/inflammation linked to an AT1-Hsp70-iNOS counterbalance axis (graphical overview). More specifically, Alli may exert a key protective role in neurological disorders as well as the development of neurodegenerative diseases. To highlight, we demonstrated also whether this counterbalance axis is associated with mitochondrial dysfunctions.

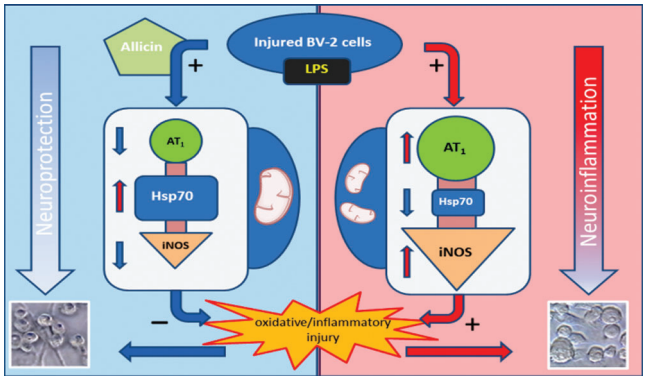

Graphical Overview. A new proposed neuroprotective mechanism of allicin during the neuroinflammatory process could be related to changes in the levels and iNOS-Hsp70-AT1 protein-protein interactions.

Acknowledgement: The authors are grateful for the collaboration and predisposition (BV-2 cells, equipment, and experimental protocols) to Dr. Vicente Lahera and the staff of the Department of Physiology. School of Medicine, Complutense University, Madrid, Spain. Also, the authors are grateful to Feres José Mocayar Marón (School of Medicine, Cuyo National University, Mendoza, Argentina) for the manuscript critical reading.

Availability of Data and Materials: All data generated or analysed during this study are included in this article.

Funding Statement: This study was funded by grants from Secretaría de Ciencia, Técnica y Postgrado, Universidad Nacional de Cuyo, and from ANPCyT (Agencia Nacional de Promoción de la Ciencia y la Tecnología, grant number PICT 2016-4541), both awarded to W. Manucha.

Conflicts of Interest: The authors declare that they have no conflicts of interest with the contents of this article.

References

Brown GC, Vilalta A (2015). How microglia kill neurons. *Brain Research* **1628**: 288–297. DOI 10.1016/j.brainres.2015.08.031.

Chabrier PE, Demerlé-Pallardy C, Auguet M (1999). Nitric oxide synthases: targets for therapeutic strategies in neurological

diseases. *Cellular and Molecular Life Sciences* **55**: 1029–1035. DOI 10.1007/s000180050353.

Cui T, Liu W, Chen S, Yu C, Li Y, Zhang J-Y (2020). Antihypertensive effects of allicin on spontaneously hypertensive rats via vasorelaxation and hydrogen sulfide mechanisms. *Biomedicine & Pharmacotherapy* **128**: 110240. DOI 10.1016/j.biopha.2020.110240.

Farooqui T, Farooqui AA 2018. Chapter 16—Neuroprotective effects of garlic in model systems of neurodegenerative diseases. In: Farooqui T, Farooqui AA, eds. *Role of the Mediterranean Diet in the Brain and Neurodegenerative Diseases. Academic Press, 253–269.*

Fernández-Arjona M D M, Grondona J A M, Granados-Durán P, Fernández-Llebrez P, López-Ávalos M D D (2017). Microglia morphological categorization in a rat model of neuroinflammation by hierarchical cluster and principal components analysis. *Frontiers in Cellular Neuroscience* **11**: 121. DOI 10.3389/fncel.2017.00235.

García IM, Altamirano L, Mazzei L, Fornés M, Cuello-Carrión FD, Ferder L, Manucha W (2014). Vitamin D receptor-modulated Hsp70/AT1 expression may protect the kidneys of SHRs at the structural and functional levels. *Cell Stress and Chaperones* **19**: 479–491. DOI 10.1007/s12192-013-0474-3.

García IM, Mazzei L, Benardón ME, Oliveros L, Cuello-Carrión FD, Gil Lorenzo A, Manucha W, Vallés PG (2012). Caveolin-1–eNOS/Hsp70 interactions mediate rosuvastatin antifibrotic effects in neonatal obstructive nephropathy. *Nitric Oxide* **27**: 95–105. DOI 10.1016/j.niox.2012.05.006.

Trejo EG, Buendía AA, Reyes OS, Arroyo FG, García R A A, Mendoza M D L, Tapia E, Lozada L S, Alonso H O (2017). The beneficial effects of allicin in chronic kidney disease are comparable to losartan. *International Journal of Molecular Sciences* **18**: 1980. DOI 10.3390/ijms18091980.

González R, Camargo A, Burba J (2007). Obtention of a quantitative secondary standard for allicin synthesis and purification. *Revista de la Facultad de Ciencias Agrarias* **39**: 61–70.

Goracci G, Ferrini M, Nardicchi V (2010). Low molecular weight phospholipases A2 in mammalian brain and neural cells: Roles in functions and dysfunctions. *Molecular Neurobiology* **41**: 274–289. DOI 10.1007/s12035-010-8108-6.

Gruhlke MCH, Antelmann H, Bernhardt J, Kloubert V, Rink L, Slusarenko AL (2019). The human allicin-proteome: S-thioallylation of proteins by the garlic defence substance allicin and its biological effects. *Free Radical Biology and Medicine* **131**: 144–153. DOI 10.1016/j.freeradbiomed.2018.11.022.

Ho SC, Su MS (2014). Evaluating the anti-neuroinflammatory capacity of raw and steamed garlic as well as five organosulfur compounds. *Molecules* **19**: 17697–17714. DOI 10.3390/molecules191117697.

Ilić D, Nikolić V, Stanković M, Nikolić L, Stanojević L, Mladenović-Ranisavljević I, Šmelcerović A (2012). Transformation of synthetic allicin: The influence of ultrasound, microwaves, different solvents and temperatures, and the products isolation. *Scientific World Journal* **2012**: 561823. DOI 10.1100/2012/561823.

Kettenmann H, Hanisch UK, Noda M, Verkhratsky A (2011). Physiology of Microglia. *Physiological Reviews* **91**: 461–553. DOI 10.1152/physrev.00011.2010.

Kong X, Gong S, Su L, Li C, Kong Y (2017). Neuroprotective effects of allicin on ischemia-reperfusion brain injury. *Oncotarget* **8**: 104492–104507. DOI 10.18632/oncotarget.22355.

Labandeira-Garcia JL, Rodríguez-Perez AI, Garrido-Gil P, Rodriguez-Pallares J, Lanciego JL, Guerra MJ (2017). Brain renin-angiotensin system and microglial polarization: Implications for aging and neurodegeneration. *Frontiers in Aging Neurosciences* **9**: 1432. DOI 10.3389/fnagi.2017.00129.

Lawson L, Hughes B (1992). Characterization of the formation of allicin and 342 other thiosulfinates from garlic. *Planta Medica* **58**: 345–350. DOI 10.1055/s-2006-961482.

Liu SG, Ren PY, Wang GY, Yao SX, He KJ (2015). Allicin protects spinal cord neurons from glutamate-induced oxidative stress through regulating the heat shock protein 70/inducible nitric oxide synthase pathway. *Food & Function* **6**: 320–329. DOI 10.1039/c4fo00761a.

Locatelli DA, Altamirano JC, Luco JM, Norlin R, Camargo AB (2014). Solid phase microextraction coupled to liquid chromatography. Analysis of organosulphur compounds avoiding artifacts formation. *Food Chemistry* **157**: 199–204. DOI 10.1016/j.foodchem.2014.02.010.

Lonnie M, Laurie I, Myers M, Horgan G, Russell WR, Johnstone AM (2020). Exploring health-promoting attributes of plant proteins as a functional ingredient for the food sector: a systematic review of human interventional studies. *Nutrients* **12**: 2291. DOI 10.3390/nu12082291.

Lv R, Mao N, Wu J, Lu C, Ding M, Gu X, Wu Y, Shi Z (2015). Neuroprotective effect of allicin in a rat model of acute spinal cord injury. *Life Sciences* **143**: 114–123.

Manucha W (2017). Mitochondrial dysfunction associated with nitric oxide pathways in glutamate neurotoxicity. *Clínica e Investigación en Arteriosclerosis* **29**: 92–97. DOI 10.1016/j.arteri.2016.04.002.

Manucha W, Vallés PG (2008). Cytoprotective role of nitric oxide associated with Hsp70 expression in neonatal obstructive nephropathy. *Nitric Oxide* **18**: 204–215. DOI 10.1016/j.niox.2008.01.005.

Martínez-Martínez E, Rodríguez C, Galán M, Miana M, Jurado-López R, Bartolomé MV, Luaces M, Islas F, Martínez-González J, López-Andrés N, Cachofeiro V (2016). The lysyl oxidase inhibitor (β-aminopropionitrile) reduces leptin profibrotic effects and ameliorates cardiovascular remodeling in diet-induced obesity in rats. *Journal of Molecular and Cellular Cardiology* **92**: 96–104. DOI 10.1016/j.yjmcc.2016.01.012.

Mazzei L, García IM, Cacciamani V, Benardón ME, Manucha W (2010). WT-1 mRNA expression is modulated by nitric oxide availability and Hsp70 interaction after neonatal unilateral ureteral obstruction. *BIOCELL* **34**: 121–132.

Mocayar Marón FJ, Camargo AB, Manucha W (2020). Allicin pharmacology: common molecular mechanisms against neuroinflammation and cardiovascular diseases. *Life Sciences* **249**: 117513. DOI 10.1016/j.lfs.2020.117513.

Nakamura T, Lipton SA (2007). S-Nitrosylation and uncompetitive/fast off-rate (UFO) drug therapy in neurodegenerative disorders of protein misfolding. *Cell Death & Differentiation* **14**: 1305–1314. DOI 10.1038/sj.cdd.4402138.

O'Beirne GB, Williams DC (1988). The subcellular location in rat kidney of the peripheral benzodiazepine acceptor. *European Journal of Biochemistry* **175**: 413–421. DOI 10.1111/j.1432-1033.1988.tb14211.x.

Pchelina SN, Emel'ianov AK, Usenko TS (2014). Molecular basis of Parkinson's disease linked with mutations in the LRRK2 gene. *Molekuliarnaia Biologiia* **48**: 3–14.

Pinazo-Durán MD, Zanón-Moreno V, Gallego-Pinazo R, García-Medina JJ (2015). Chapter 6-Oxidative stress and mitochondrial failure in the pathogenesis of glaucoma

neurodegeneration, In: *Progress in Brain Research. vol.* **220**, Elsevier, 127–153.

Prado NJ, Casarotto M, Calvo JP, Mazzei L, Ponce Zumino AZ, García IM, Cuello-Carrión FD, Fornés MW, Ferder L, Diez ER, Manucha W (2018). Antiarrhythmic effect linked to melatonin cardiorenal protection involves AT1 reduction and Hsp70-VDR increase. *Journal of Pineal Research* **65**: e12513. DOI 10.1111/jpi.12513.

Qian YQ, Feng ZH, Li XB, Hu ZC, Xuan JW, Wang X, Xu HC, Chen JX (2018). Downregulating PI3K/Akt/NF-κB signaling with allicin for ameliorating the progression of osteoarthritis: *in vitro* and vivo studies. *Food & Function* **9**: 4865–4875. DOI 10.1039/C8FO01095A.

Rajdev S, Sharp FR (2016). Stress proteins as molecular markers of neurotoxicity. *Toxicologic Pathology* **28**: 105–112. DOI 10.1177/019262330002800113.

Saavedra JM (2017). Beneficial effects of angiotensin II receptor blockers in brain disorders. *Pharmacological Research* **125**: 91–103. DOI 10.1016/j.phrs.2017.06.017.

Sardari K, Mirshahi A, Maleki M, Aslani MR, Najar Barjasteh M (2006). Effects of topical allicin on second-intention wound healing in dogs (histological aspects). *Comparative Clinical Pathology* **15**: 98–102. DOI 10.1007/s00580-006-0616-4.

Smaili SS, Ureshino RP, Rodrigues L, Rocha KK, Carvalho JT, Oseki KT, Bincoletto C, Lopes GS, Hirata H (2011). The role of mitochondrial function in glutamate-dependent metabolism in neuronal cells. *Current Pharmaceutical Design* **17**: 3865–3877. DOI 10.2174/138161211798357782.

Son M, Elliott JL (2014). Mitochondrial defects in transgenic mice expressing Cu, Zn superoxide dismutase mutations: The role of copper chaperone for SOD1. *Journal of the Neurological Sciences* **336**: 1–7. DOI 10.1016/j.jns.2013.11.004.

Ho SC, Su MS (2014). Evaluating the anti-neuroinflammatory capacity of raw and steamed garlic as well as five organosulfur compounds. *Molecules* **19**: 17697–17714. DOI 10.3390/molecules191117697.

Takarada T, Fukumori R, Yoneda Y (2013). Mitochondrial uncoupling protein-2 in glutamate neurotoxicity. *Folia Pharmacologica Japonica* **142**: 13–16. DOI 10.1254/fpj.142.13.

Toma VA, Tigu AB, Farcaş AD, Sevastre B, Taulescu M, Gherman AMR, Roman I, Fischer-Fodor E, Pârvu M (2019). New aspects towards a molecular understanding of the allicin immunostimulatory mechanism via Colec12, MARCO, and SCARB1 receptors. *International Journal of Molecular Sciences* **20**: 3627. DOI 10.3390/ijms20153627.

Toygar I, Tureyen A, Demir D, Cetinkalp S (2020). Effect of allicin on wound healing: an experimental diabetes model. *Journal of Wound Care* **29**: 388–392. DOI 10.12968/jowc.2020.29.7.388.

Uhlemann R, Gertz K, Boehmerle W, Schwarz T, Nolte C, Freyer D, Kettenmann H, Endres M, Kronenberg G (2016). Actin dynamics shape microglia effector functions. *Brain Structure and Function* **221**: 2717–2734. DOI 10.1007/s00429-015-1067-y.

Urrutia PJ, Mena NP, Núñez MT (2014). The interplay between iron accumulation, mitochondrial dysfunction, and inflammation during the execution step of neurodegenerative disorders. *Frontiers in Pharmacology* **5**: 81. DOI 10.3389/fphar.2014.00038.

Wang X, Ch Zhang, Ch Chen, Guo Y, Meng X, Ch Kan (2018). Allicin attenuates lipopolysaccharide-induced acute lung injury in neonatal rats via the PI3K/Akt pathway. *Molecular Medicine Reports* **17**: 6777–6783.

Xiang Q, Li XH, Yang B, Fang Jia XX, Ren J, Dong J, Ou-Yang YC, Wang C, GC. 2017. (2017). Allicin attenuates tunicamycin-induced cognitive deficits in rats via its synaptic plasticity regulatory activity. *Iranian Journal of Basic Medical Sciences* **20**: 676–682. DOI 10.22038/IJBMS.2017.8837.

Yu X, Murao K, Imachi H, Cao W-M, Li J, Matsumoto K, Nishiuchi T, Ahmed RAM, Wong NCW, Kosaka H, Unterman TG, Ishida T (2007). Regulation of scavenger receptor class BI gene expression by angiotensin II in vascular endothelial cells. *Hypertension* **49**: 1378–1384. DOI 10.1161/HYPERTENSIONAHA.106.082479.

Zhang C, He X, Sheng Y, Yang C, Xu J, Zheng S, Liu J, Xu W, Luo Y, Huang K (2020). Allicin-induced host-gut microbe interactions improves energy homeostasis. *FASEB Journal* **34**: 10682–10698. DOI 10.1096/fj.202001007R.

Zhang H, Wang P, Xue Y, Liu L, Li Z, Liu Y (2018). Allicin ameliorates cognitive impairment in APP/PS1 mice via suppressing oxidative stress by blocking JNK signaling pathways. *Tissue and Cell* **50**: 89–95. DOI 10.1016/j.tice.2017.11.002.

Zhang M, Pan H, Xu Y, Wang X, Qiu Z, Jiang L (2017). Allicin decreases lipopolysaccharide-induced oxidative stress and inflammation in human umbilical vein endothelial cells through suppression of mitochondrial dysfunction and activation of Nrf2. *Cellular Physiology and Biochemistry* **41**: 2255–2267. DOI 10.1159/000475640.

Zheng YL, Cai WW, Yan GZ, Xu YZ, Zhang M (2014). Allicin protects against lipopolysaccharide-induced acute lung injury by up-regulation of claudin-4. *Tropical Journal of Pharmaceutical Research* **13**: 1063–1069. DOI 10.4314/tjpr.v13i7.8.

Zlatković J, Bernardi RE, Filipović D (2014). Protective effect of Hsp70i against chronic social isolation stress in the rat hippocampus. *Journal of Neural Transmission* **121**: 3–14. DOI 10.1007/s00702-013-1066-1.